Title

α1-Antitrypsin derived SP16 peptide demonstrates efficacy in rodent models of acute and neuropathic pain

Journal

The FASEB Journal, 36(1)

ISSN

0892-6638

Authors

Wang, Zixuan
Martellucci, Stefano
Van Enoo, Alicia
et al.

Publication Date

2022

DOI

10.1096/fj.202101031rr

Published in final edited form as:

FASEB J. 2022 January ; 36(1): e22093. doi:10.1096/fj.202101031RR.

α1-Antitrypsin derived SP16 peptide demonstrates efficacy in rodent models of acute and neuropathic pain

Zixuan Wang[1], **Stefano Martellucci**[1], **Alicia Van Enoo**[1,2], **Dana Austin**[3], **Cohava Gelber**[3], **Wendy M. Campana**[1,2,4]

[1]Department of Anesthesiology, School of Medicine, University of California, San Diego, La Jolla CA, 92093-0629 USA;

[2]Program in Neurosciences, University of California, San Diego, La Jolla CA 92093, USA;

[3]Serpin Pharma, Manassas, VA, 20109, USA;

[4]San Diego Veterans Administration Health Care System, CA, 92161, USA.

Abstract

SP16 is an innovative peptide derived from the carboxyl-terminus of α1-Antitrypsin (AAT), corresponding to residues 364–380, and contains recognition sequences for the low-density lipoprotein receptor-related protein-1 (LRP1). LRP1 is an endocytic and cell-signaling receptor that regulates inflammation. Deletion of *Lrp1* in Schwann cells increases neuropathic pain; however, the role of LRP1 activation in nociceptive and neuropathic pain regulation remains unknown. Herein, we show that SP16 is bioactive in sensory neurons *in vitro*. Neurite length and regenerative gene expression were increased by SP16. In PC12 cells, SP16 activated Akt and ERK1/2 cell-signaling in an LRP1-dependent manner. When formalin was injected into mouse hindpaws, to model inflammatory pain, SP16 dose-dependently attenuated nociceptive pain behaviors in the early and late phases. In a second model of acute pain using capsaicin, SP16 significantly reduced paw licking in both male and female mice ($P<0.01$) similarly to enzymatically inactive tissue plasminogen activator, a known LRP1 interactor. SP16 also prevented development of tactile allodynia after partial nerve ligation and this response was sustained for nine days ($P<0.01$). Immunoblot analysis of the injured nerve revealed decreased CD11b ($P<0.01$) and Toll-like Receptor-4 ($P<0.005$). In injured DRGs, SP16 reduced CD11b+ cells ($P<0.05$) and GFAP ($P<0.005$), indicating that inflammatory cell recruitment and satellite cell activation were inhibited. In conclusion, administration of SP16 blocked pain-related responses in three distinct pain models, suggesting efficacy against acute nociceptive, inflammatory, and neuropathic pain. SP16 also attenuated innate immunity in the PNS. These studies identify SP16 as a potentially effective treatment for pain.

Correspondence should be addressed to Dr. Wendy M Campana, University of California San Diego, Department of Anesthesiology, 9500 Gilman Drive, La Jolla, CA, 92093-0629. wcampana@health.ucsd.edu.

AUTHOR CONTRIBUTIONS

Z.W., D.A., C.G. and W.M.C. conceived of and designed the overall study. Z.W., A.V., S.M., and W.M.C. performed research. C.G. contributed SP16. Z.W., A.V., S.M., and W.M.C. analyzed data. Z.W. and W.M.C. wrote the initial draft of the manuscript. W.M.C. revised the manuscript. S.M., Z.W., C.G., D.A and W.M.C. edited the manuscript.

CONFLICT OF INTEREST

Dr. Campana serves on the company's Scientific Advisory Board for Serpin Pharma. The terms of this arrangement have been reviewed and approved by the University of California, San Diego in accordance with its conflict of interest policies.

Keywords

LRP1; nociception; neuropathic pain; SP16; neuroinflammation; peripheral nerve injury

1 | INTRODUCTION

Peripheral nerve injury (PNI) resulting from metabolic, chemotherapy or trauma often results in chronic pain. Neuropathic pain is characterized by evoked (allodynia, hyperalgesia) and spontaneous pain-like symptoms (1). The symptoms may be severe including paresthesia, tingling, numbness and burning sensations. Other than short term symptomatic relief, few therapeutic options are available and include steroids, local anesthetics, antidepressants, anti-seizures drugs, and opioids, which are reserved for severe pain. All these treatments aim at temporarily reducing pain to manageable levels; however, all can cause side effects and addiction (2,3) and do not promote healing of damage nerves. Accordingly, there is an unmet clinical need for novel and innovative pain treatments to prevent the transition from acute to chronic pain.

Recently, SP16, a small peptide derived from the C-terminus of α1-Antitrypsin (AAT) was synthesized based on the structure function of LRP1 (4) that contains putative LRP1 recognition sequences (5–10) and no restrictive structure. In murine monocytes, SP16 blocked NFκB activation and IL-1β release induced by LPS or GP96 that was LRP1-dependent *in vitro* (11). SP16 also demonstrated potent anti-inflammatory activities, reduced cardiomyocyte death, and infarct-sparing effects in a mouse model of acute myocardial ischemia-reperfusion injury (AMI) (11). These results summarized by Potere *et al.*, 2019 (12) revealed the potential translational value of LRP1 as a novel therapeutic target in AMI. Accordingly, SP16 showed safety and tolerability in in a Phase 1 clinical trial of healthy adult volunteers (13).

Considerable evidence indicates that membrane-anchored low-density lipoprotein receptor-related protein-1 (LRP1) is potently anti-inflammatory (14,15). Engagement of the LRP1 and its co-receptor systems antagonize inflammatory cytokines and Toll-like receptors (TLRs) including TLR4, TLR2 and TLR9 (16), suggesting that it plays a key role in innate immunity. This is important because TLRs are emerging as a therapeutic target for persistent pain states (17,18). Conditional deletion of LRP1 in glia induces neuroinflammation. In microglia, loss of LRP1 exacerbates experimental autoimmune encephalomyelitis in mice (19) probably reflecting loss of the membrane-anchored form of the receptor. It is also possible that deletion of LRP1 prevents the production of the pro-inflammatory soluble ectodomain of LRP1 (20) which is notably present at increased levels in plasma from patients with painful rheumatoid arthritis (21,22). In Schwann cells (SC), genetic deletion of LRP1 increases the extent and magnitude of neuropathic pain before and after injury (23). Although the loss of LRP1 function appears to promote inflammation and neuropathic pain, it is not known whether the gain of LRP1 activation alleviate nociceptive and neuropathic pain states (24).

Herein, we identify SP16 as a significant regulator of acute nociceptive, inflammatory, and neuropathic pain. SP16 replicated the neurite extension activity previously shown by other

LRP1 agonists (25–28). We demonstrate that Akt and ERK1/2 cell-signaling is activated by SP16 and blocked by inhibiting SP16 binding with receptor associated protein (RAP) or by LRP1 gene silencing. SP16 modulates primary afferent activity by blocking the activation of nociceptors and inflammatory related nociception after intraplantar capsaicin or formalin. In a neuropathic pain model, SP16 prevented the development of mechanical hypersensitivity that was associated with reduced inflammatory cell recruitment into the injured nerve while reducing levels of TLR4. In addition, activation of satellite cells and decreased inflammatory cells were identified in injured DRGs treated with SP16. SP16 emerges as a potent LRP1 interactor that regulates acute and neuropathic pain states. SP16 may modulate the transition from acute to chronic pain and thereby, have significant translational potential as a pain alleviating therapeutic.

2 | MATERIALS AND METHODS

2.1 | Animals

Male Sprague Dawley rats (170–200 g; 8–12 weeks old) and C57BL/6J mice (25 g; male and female, 8–12 weeks old) were purchased from Envigo and Jackson Laboratory, respectively. All animal experiments were approved by the Institutional Animal Care and Use Committee at University of California, San Diego. All rat and mice were housed with a 12hrs:12hrs light: dark cycle with ad libitum access to food and water.

2.2 | Reagents

SP16 (Ac-VKFNKPFVFLNleIEQNTK-NH2) was provided from Serpin Pharma (Manassas, VA, USA) as previous described (11). Briefly, peptides were synthesized by CPC Scientific Inc (Sunnyvale, CA) with purity >95% as verified by high performance liquid chromatography and mass spectroscopy. Recombinat human EI-tPA was purchased from Molecular Innovations (Novi, MI, US). NGF-β was purchased from Sigma (St. Louis, MO, USA). RAP was expressed as a glutathione-S-transferase (GST)-fusion protein (GST-RAP) as previously described by us and others (29, 30).

2.3 | Neurite outgrowth in primary cultures of adult DRG neurons

Primary DRG neurons were isolated from adult male Sprague Dawley rats and cultured as previously described for mice with modifications (26). The DRGs were stripped of their roots and collected in Hanks Buffered Salt Solution (HBSS) on ice. DRGs were enzymatically digested and approximately 4000 DRG neurons were plated in each well of a 12-well tissue culture plates (Thermo Fisher Scientific, Waltham, MA, USA). All DRG neurons were cultured at 37 °C in 5% CO_2 for 54 hrs in DMEM/F12 containing 2% B27 and 1%FBS with vehicle or SP16 (0–500 ng/mL) added every 24 hrs. Primary cultured DRG neurons were imaged by phase contrast and the viability of cells was assessed by Trypan blue. Primary DRG neurons were cultured, fixed in 4% paraformaldehyde, and immunofluorescence was performed using a mouse anti-βIII-tubulin primary antibody (Promega, Madison, WI, USA; cat#G7121, 1:250) and then with Alexa Fluor-488 anti-mouse antibody (Life Technologies, Carlsbad, CA USA) as secondary antibody. DRG neurons were imaged at 20x and 40x manually, and the longest neurite length per cell was measured in 11 images from multiple wells and separate experiments. Approximately 222

and 144 neurons were measured in SP16 and control groups, respectively. Quantification was performed in a blinded manner. For all neurite outgrowth measurements, at least 6 individual experiments were performed in duplicate.

2.4 | Cell signaling analysis

Rat PC12 cells were purchased from ATCC (CRL-1721). PC12 cells were maintained in high glucose DMEM (Gibco, USA) containing 10% heat-inactivated FBS (Gibco, USA), 5% HyClone heat-inactivated horse serum (Cytiva, USA), penicillin (100 units/ml) and streptomycin (1mg/ml) in 6-well plates that were pre-coated with 0.01 mg/ml type IV collagen (Sigma-Aldrich, St. Louis, USA). Cells were transferred to serum-free medium (SFM) 4 hrs prior to adding effectors, and then treated with SP16 (2.4, 24 or 240 nM); EI-tPA (12 nM), NGF (0.36 nM), or vehicle (PBS) for 10 mins. In some cases, cells were pre-incubated with the competitive antagonist of LRP1, GST-RAP (150 nM) for 15 min or electroporated using the Rat Neuron Nucleofector Amaxa Kit (Lonza Biosciences) and incubated with siRNA to silence LRP1 expression (siLRP1; M-094191-01-0010, Dharmacon) for 48 hrs. Control cells were transfected with non-targeting control (NTC) siRNA (NTC; D-001810-10-05, Dharmacon). Cells were rinsed with ice-cold PBS and proteins were extracted in RIPA buffer (20 mM sodium phosphate, 150 mM NaCl, pH 7.4, 1% Triton X-100, 0.5% sodium deoxycholate, 0.1% SDS) supplemented with protease and phosphatase inhibitors (Roche Diagnostics, USA). After 30 mins on ice, lysates were centrifuged at 15,000 × g for 5 mins, supernatant collected and stored at −20 °C. Equal amounts of protein from cell lysates (20 μg), as determined by BCA Protein Assay (Thermo Fisher Scientific, Waltham, MA, USA), were subjected to 10% SDS-PAGE and electro-transferred to nitrocellulose membranes. The membranes were blocked with 5% nonfat dried milk and then incubated with primary anti-phospho-AKT (Cell Signaling Technology, Danvers, MA; cat#9271S; 1:1000), anti-phospho-ERK1/2 (Cell Signaling Technology, Danvers, MA, USA; cat#9101S; 1:1000), anti-LRP1 (Cell Signaling Technology, Danvers, MA, USA; cat#64099S; 1:1000) or anti total-ERK1/2 (Cell Signaling Technology, Danvers, MA; cat#91012S; 1:1000). Immunoblots were developed using Radiance, Radiance Q and Radiance Plus chemiluminescent substrates and imaged using a BioRad ChemiDoc Imaging System, Bio-Rad, Hercules, CA, USA.

2.5 | RT-qPCR

RNA was isolated from DRG cultures using the NucleoSpin RNA kit (MachereyNagel, Duren, GER) and reverse-transcribed using the iScript cDNA synthesis kit (Bio-Rad, Hercules, CA, USA). qPCR was performed using TaqMan gene expression products (Thermo Fisher Scientific, Waltham, MA, USA) for GAP-43 (Rn01474579), LRP1 (Rn01503901_m1) and GAPDH (Rn99999916_s1). Amplification was performed with CFX Connect Real-Time PCR detection system (Bio-Rad, Hercules, CA, USA). The relative change in mRNA expression was calculated using the $2^{\Delta\Delta CT}$ method with GAPDH mRNA as an internal normalizer as we described previously (31).

2.6 | Intraplantar formalin and capsaicin models

Male mice (n=33) were acclimated to the behavior testing facility for at least 60 min. Mice were randomized into four groups SP16 (0.02, 0.2 and 2 μg/g) or vehicle were administered

subcutaneously. After 1 hr, 20 μL of 2.5% formalin was injected subcutaneously into the plantar area of left hind paw. Immediately after formalin injection, mice are placed in a Plexiglas box (22 × 22 × 14 cm). Two observers, blinded to treatments, recorded the total amount of time mice spent on licking and flinching the left hind paw every 5 minutes over a one-hour period. To quantify the formalin response, activity during early phase (0–10 mins) and later phase (15–50 mins) were examined separately.

For the capsaicin studies, male (n=41) and female (n=37) mice were acclimated to the behavior testing facility for at least 1 hr. Capsaicin was dissolved in 20% (2-Hydroxypropyl)-β-cyclodextrin (Sigma-Aldrich, St. Louis, USA) solution. This vehicle concentration solubilized the capsaicin and did not induce a behavioral response when administered alone. One hour prior to intraplantar injections, vehicle, SP16 (2 μg/g; s.c.) or enzymatically inactive tPA (EI-tPA; 2 μg/g i.v.) were administered. Subsequently, 10 μL of 2 μg/μL capsaicin solution was injected into the plantar area of left hind paw. Immediately after capsaicin injection, mice were place in a plexiglass box. Two observers, blinded to treatments, recorded the time spent licking and flinching the left hind paw over 10 mins.

2.7 | Neuropathic pain model

Mice (n=30) were randomly assigned to two different groups: SP16 (2 μg/g; s.c. 100 μl) and vehicle (H_20 s.c. 100 μl). Mice were treated 1 hr prior to partial nerve ligation (PNL) and then daily at least 1 hr prior to behavior testing for 2 weeks. PNL studies were performed as previously described (32,) and adapted for mice (23). Male mice were anesthetized with 3% isoflurane (Vetone, USA) in 1.5L/min oxygen (Praxair, USA) and maintained with 2.5% isoflurane. An incision was made along the long axis of the femur. The sciatic nerve was exposed at mid-thigh level by separating the biceps femoris and the gluteus superficialis and then carefully cleared of surrounding connective tissue. A 9–0 nylon suture (Ethicon, Inc., Somerville, NJ, USA) was inserted into the nerve and ligated so that the one-third to one-half of the nerve was included. The muscle and skin layers were closed using Reflex7 7 mm stainless steel wound clips (CellPoint Scientific, Inc., Gaithersburg, MD, USA). For behavior testing, mice were acclimated, and baseline tested for one week prior to PNL. Mechanical sensitivity (tactile allodynia) was tested by applying 0.04 to 4 g Von Frey filaments (Stoelting, Wood Dale IL, USA) to the plantar surface of the ipsilateral hind paw. Filaments were presented in a consecutive fashion either ascending or descending using the up-down method as previously described (33) and modified for mice (23,34). The filament that caused paw withdrawal 50% of the time (the 50% PWT) was determined. Tactile allodynia was tested on days 2, 4, 9, 11, and 14 days following PNL. Results were averaged and subjected to statistical analysis. All experiments were performed by an investigator blinded to mouse identity.

2.8 | Immunoblots of sciatic nerve

Sciatic nerves were harvested 2 days after PNL to identify early molecular and cellular changes. Approximately 0.5 cm of sciatic nerve was collected distal from the ligation site. Ipsilateral and contralateral nerves were collected. Nerves were lysed in RIPA buffer and equal amounts of protein (20 μg) from nerves lysates, as determined by BCA Protein Assay (Bio-Rad, Hercules, CA, USA), were subjected to 10% SDS-PAGE and electro-

transferred to nitrocellulose membranes. The membranes were blocked with 5% nonfat dried milk and then incubated with anti-TLR4(CD284)/MD2 (BioLegend, San Diego, CA, USA; cat#117601, 1:1000), anti-CD11b (Abcam, Cambridge, MA, USA, cat#Ab1333357) and anti-β-actin (Cell Signaling Technology, Danvers, MA, USA; cat#1:1000). Primary antibodies were detected with HRP-conjugated species-specific secondary antibodies (Cell Signaling Technology, Danvers, MA, USA; cat#7076S or 4S; 1:5000). Immunoblots were developed using SuperSignal West Pico PLUS chemiluminescent substrate (Thermo Fisher Scientific, Waltham, MA, USA), and the Protec Ecomax X-ray film processor. Densitometry analysis was performed using Image J software (U. S. National Institutes of Health, Bethesda, MD, USA).

2.9 | Immunohistochemistry of DRGs

DRGs were embedded in paraffin. For IHC studies, 4 μm thick DRG tissue sections were immunostained for CD11b (Abcam, Cambridge, MA, USA, cat#Ab1333357; 1:4500) or GFAP (Dako, Santa Clara, CA, USA; cat#$Z0334; 1:4000). Slides were immunostained using a Ventana Discovery Ultra (Ventana Medical Systems, Oro, Az, USA). Antigen retrieval was performed using CC1 (tris-based; pH 8.5) for 40 mins at 95 °C. The primary antibodies CD11b and GFAP was incubated with the slides for 32 mins at 37 °C. The secondary antibody, OmniMap anti-HRP (Ventana Medical Systems, Oro, Az, USA; cat#760–4311), was incubated on the sections for 12 min at 37 °C. Antibodies were visualized using diaminobenzidine as a chromogen followed by hematoxylin as a counterstain. Slides were rinsed, dehydrated through alcohol and xylene and cover slipped. Light microscopy was performed using a Leica DFC420 microscope with Leica Imaging Software 2.8.1 (Leica Biosystems, Vista, CA, USA).

2.10 | Statistical Analysis

Statistical analysis was performed using GraphPad Prism (GraphPad Prism version 9.1.2 for Mac, GraphPad Software, San Diego, CA, USA). All results are expressed as the mean ± S.E.M. Comparisons between two groups were performed using two-tailed unpaired T-tests. A non-parametric Mann-Whitney U test was used when the variance in the two populations were significantly different. When we compared greater than two groups, a one-way ANOVA and Tukey's *post hoc* test was performed or in the case of non-parametric data, we utilized the Kruskal-Wallis test. Measurements of neuropathic pain, in which we collected multiple observations in individual mice over time, were analyzed by repeated-measures ANOVA with a Sidak's *post hoc* test. $P<0.05$ was considered statistically significant.

3 | RESULTS

3.1 | Primary adult sensory neurons sprout in response to SP16

To determine whether SP16 also possessed bioactivity in sensory neurons, we treated primary adult rat DRG neurons with SP16 for up to 96 hrs. Within 48 hrs, phase contrast images of DRG neuronal cultures revealed that SP16 induced greater neuronal survival and neurite sprouting compared to untreated controls (Figure 1A). After 72 and 96 hrs in culture, the neuronal networks became extensive and continued to show a greater survival of neuronal cell bodies and neurite extensions.

To specifically identify neuronal cell bodies, we performed immunofluorescence studies with βIII-tubulin. Primary adult DRG neuron cultured on poly-L-lysine (PLL) and laminin showed basal levels of sprouting when treated with vehicle after 54 hrs (Figure 1B). In contrast, cultured DRG neurons treated with SP16 showed significant levels of sprouting that included increases in both branching and length after 54 hrs. Quantification of the longest neurite indicated that SP16 was significantly neurotrophic (Figure 1C). RT-qPCR analysis of a regenerative associated gene, growth associated protein, GAP-43, demonstrated that SP16 increased GAP-43 mRNA compared to vehicle-treated neurons (Figure 1D).

3.2 | SP16 activates LRP1 dependent cell signaling

Previously, it was shown that LRP1 ligands, such as EI-tPA, robustly activate cell survival signaling in neurons and SCs (20–23), however the effects of SP16 were unknown. To begin, we added several concentrations of SP16 to cultured PC12 cells for 10 min. SP16 activated phospho-ERK1/2 at concentrations as low as 24 nM (Figure 2A). Next, we added SP16 to PC12 cells over time. SP16 robustly activated ERK1/2 from 5–30 min (Figure 2B). SP16 activation of ERK1/2 at 10 min was similar to the known LRP1 interactor, EI-tPA (35). EI-tPA is a derivative of tissue-type plasminogen activator (tPA), a protease that is an activator of fibrinolysis, and is globally approved drug for treating non-hemorrhagic stroke (36). Next, we silenced LRP1 expression with siRNA (siLRP1). PC12 cells transfected with siLRP1 showed significantly decreased (70%) expression of LRP1 mRNA compared with cells transfected with NTC siRNA for 48 h (Figure 2C). LRP1 protein also was significantly reduced after 48 hrs (Figure 2D). When PC12 cells transfected with NTC siRNA were treated with SP16, ERK1/2 was robustly activated. EI-tPA also robustly activated ERK1/2, as anticipated. In contrast, ERK1/2 was not activated by SP16 or EI-tPA in cells transfected with LRP1-specific siRNA (Figure 2E). SP16 also activated Akt and EKR1/2 in PC12 cells after 10 mins that was blocked by the addition of the 39 kDa LRP1 antagonist receptor associated protein, RAP (150 nM), as expected for any LRP1-dependent agonist (Figure 2F). NGF also activated ERK1/2, as anticipated, and served as a cell signaling control. Collectively, these data support that SP16 is bioactive in sensory neurons and sensory-like neurons via a LRP1 dependent pathway.

3.3 | SP16 modulates primary afferent input and reduces central sensitization in the later phase of the formalin test

The formalin test is a tissue injury model with an acute nociceptive first phase and an inflammatory second phase (37). It is a widely used tool to screen analgesic and anti-inflammatory pain therapeutics. We tested whether LRP1 agonism by SP16 regulated pain responses induced by intraplantar formalin (Figure 3A). SP16 (0.02, 0.2 or 2.0 μg/g) or vehicle was administered one hour prior to paw injection of 2.5% formalin solution. We initially studied preemptive administration to understand the contribution of primary afferent input in the early phase and is an approach consistent with other formalin test studies testing initial effects of novel opioids or other analgesics (37,38). Time spent licking was quantified by two blinded observers over 50 minutes. Vehicle treated mice showed the characteristic pattern of paw licking during the two phases. In the early phase (0–10 min), vehicle-treated mice robustly licked their injected hind paw for over 100 seconds. However, SP16 treated-mice demonstrated dose-dependent reductions in licking time (0.02 μg/g; 80 seconds) and

high (2 μg/g; 60 seconds). Analysis of area under the curve (AUC) revealed that both the low and high SP16 treatment groups reached statistical significance (Figure 3B). In the later phase (15–50 min), vehicle-treated mice showed peaked paw licking (90 seconds) after 25 minutes that resolved at 50 minutes, as anticipated (Figure 3A). In contrast, the highest dose of SP16 (2 μg/g) delayed the peak late phase start time to 30 min. Analysis of AUC revealed that both middle (0.2 μg/g) and high (2 μg/g) doses reduced licking time in the late phase compared to vehicle controls (Figure 3C). Our findings indicate that LRP1 activation by SP16 reduced both the nociceptive and ongoing sensitization/inflammatory phase of the formalin test.

3.4 | LRP1 ligands block acute nociception

Intraplantar injection of capsaicin, the lipophilic vanilloid compound found in “hot” chili peppers (39) binds and activates TRPV1 in nociceptive peripheral terminals (40). This induces ion influx and action potential firing associated with burning pain resulting in a licking response toward the injected paw. The acute spontaneous pain related behaviors induced by capsaicin are transient (<10 mins) with most of the activity occurring during the first 2–3 mins. Initially, we confirmed that capsaicin increased pain related behaviors in male and female mice when using 20% cyclodextrin as the vehicle for the capsaicin solution. Both male and female mice manifested a greater licking response to capsaicin injection than vehicle injection; the males tended to be slightly more sensitive (Figure 4A). Because anti-nociceptive activities have not been previously shown for any LRP1 interactor, we tested both EI-tPA and SP16. We delivered EI-tPA or SP16 systemically and one hour preemptively prior to capsaicin injection in both male and female mice. In male mice, SP16 and EI-tPA, blocked the capsaicin induced acute pain related behavior (Figure 4B). Similar effects of LRP1 agonists were observed in female mice (Figure 4C).

3.5 | SP16 inhibits the development of neuropathic pain, suppresses innate immunity and reduces inflammatory cell recruitment

Next, we tested SP16 in a neuropathic pain model, partial nerve ligation (PNL). PNL in the sciatic nerve induces mechanical hypersensitivity that can be observed within two days after injury (23). Male mice were randomly placed into groups, baselined with von Frey filaments and paw withdrawal thresholds (PWT) were recorded over one week prior to PNL. SP16 (2 μg/g) was given preemptively one hour prior to PNL and then daily for two weeks to test whether SP16 was neuroprotective. Vehicle-treated mice developed tactile allodynia by day 2 and hypersensitivity continued for 2 weeks (Figure 5A), as anticipated. In contrast, mice that were treated with SP16 did not develop mechanical hypersensitivity. Statistically, the effects of SP16 were most pronounced early after injury (day 2 and 4), nonetheless, the anti-allodynic effects of SP16 were sustained throughout day 9 post injury. These results indicate that activation of LRP1 may prevent the development of mechanical sensitivity induced by direct nerve damage.

LRP1 induces potent anti-inflammatory activity in macrophages (14), during myocardial infarction (11,12) and can regulate innate immunity (16). To determine whether SP16 modulates neuroinflammation in the injured PNS, we collected sciatic nerves from vehicle and SP16 treated groups two days after PNL. CD11b was used to identify inflammatory

cells present in the nerve. CD11b was robustly increased in nerve immediately distal to the ligation site in vehicle treated mice, as anticipated (Figure 5B). In contrast CD11b was decreased in nerves treated with SP16. Densitometric analysis revealed that CD11b was increased almost 20-fold (Figure 5C, $P<0.001$) and SP16 reduced the levels of CD11b by 10-fold ($P<0.01$). Because activation of TLR4 is associated with pain states (17), we also measured TLR4 in injured sciatic nerves. Immunoblots revealed that TLR4 is upregulated in nerve two days after PNL and that SP16 robustly down regulated TLR4 expression (Figure 5D). Densitometric analysis revealed that TLR4 increased greater than 2-fold after injury in vehicle treated mice and that SP16 completely blocked the upregulation of TLR4 (Figure 5E).

Recently, it has been shown that inflammatory cells and macrophages infiltrating into the DRGs acutely after nerve injury directly regulate chronic pain states (41–43). Accordingly, we collected L4 DRGs from mice that received vehicle or SP16 treatment two days after PNL. Immunohistochemistry was performed on transverse DRG sections to identify CD11b (Figure 6A). In PNL sections, CD11b immunoreactivity was observed in between neuronal cell bodies and around blood vessels. In contrast, transverse sections of SP16 treated nerves revealed little immunoreactivity, indicating a very low level of inflammatory cells present. Quantification of CD11B immunohistochemistry showed that SP16 treated DRGs had approximately five-fold less CD11b levels than vehicle-treated DRGs (Figure 6B). Next, we examined satellite cell activation. Satellite cells in naïve DRGs do not express GFAP, however after injury, satellite cells abundantly express GFAP (44–46). Two days after PNL, satellite cells showed robust GFAP immunoreactivity in vehicle treated DRGs. Conversely, mice that were treated with SP16 showed significantly less GFAP expression in DRGs. Quantification of GFAP immunohistochemistry revealed a 6-fold decrease in GFAP levels in SP16 treated mice (Figure 6C). These findings suggest that engagement of LRP1 reduces satellite cell activation.

4 | DISCUSSION

This study demonstrates robust efficacy of SP16, an innovative peptide, in three distinct pre-clinical mouse models that includes acute nociceptive, inflammatory, and neuropathic pain. Central to the effect of preventing mechanical hypersensitivity by SP16, was its potent anti-inflammatory activity in injured peripheral nerves. In these studies, SP16 robustly reduced the early recruitment of inflammatory cells distal to the nerve injury site and in the corresponding L3, L4 DRG early after sciatic nerve ligation. This is important as recruitment of macrophages into injured nerve and DRGs increases neuropathic pain states in many types of painful peripheral neuropathies (42,47). Our findings suggest that SP16 can delay and/or limit the infiltration of inflammatory cells and thereby regulate pain states. Further studies are needed to determine whether these SP16 regulated activities also support long term sensory nerve regeneration in painful neuropathies such as diabetic neuropathy and chemotherapy induced neuropathy.

Importantly, we show that SP16 induced cell signaling in neuron like cells is LRP1 dependent. Our findings that RAP blocked SP16 activation of Akt and ERK1/2, and that LRP1 silencing prevented SP16 activation of ERK1/2, provide convincing evidence

that LRP1 is involved in SP16 induced neuronal activities. Previous work defined SP16 as an LRP1 agonist in cardiomyocytes (11), however, the exact binding mechanism and binding affinities have yet to be determined. SP16 encompasses putative LRP1 recognition sequences. SP16 contains the pentapeptide residues 370–374-FVFLM located in the carboxyl terminal fragment of AAT that were initially implicated in LRP1 binding (4,6). Yet, whether this sequence is relevant remains unclear. Mutations in this sequence and monoclonal antibodies targeted to this region failed to decrease the internalization, binding or degradation of serpin enzyme complexes (48,49). However, SP16 also encompasses putative LRP1 recognition sequences including tandem lysine residues that could potentially interact with negatively charged amino acids in the LRP1 complement repeats (4,5). It also has hydrophobic residues exposed on the surface and these may be involved in LRP1 interactions. Critical lysine residues have been identified for other LRP1 ligands including RAP (9), α2M (8), Coagulation Factor VIII (50), and the serpin, PAI-1 (51). Furthermore, a combination of lysines and the pentapeptide sequence appear to facilitate binding to LRP1 (52). Future studies in mice with LRP1 deficient pain producing neurons and SP16 mutants lacking LRP1 recognition sequences will further define the role of LRP1 in nociceptive regulation.

In the formalin test, SP16 revealed reductions in both early and late phases, suggesting direct effects on nociceptors and an ability to antagonize acute inflammatory pain. It is possible that SP16 suppresses primary afferent input throughout the duration of formalin test since it was administered as a pre-treatment. Indeed, LRP1 is present in sensory neurons and glia in the PNS that are associated with nociceptive pain processing (26,53). Decreased nociceptive behaviors induced by SP16 in the formalin test are consistent with a drug that is considered analgesic (54). Investigating alternatives to opioids as potential pain-alleviating therapeutics is an important goal. Our initial findings also suggest, that SP16 does not behave like an NMDAR antagonist that are only capable of reducing the late phase of the formalin test when given as a pretreatment (55). Whether SP16 can block the development of central sensitization without suppressing afferent input remains to be determined. Importantly, LRP1 is also abundantly present in glia and neurons in the CNS that are directly involved or recruited into nociceptive processing. Thus, direct regulation in spinal cord and brain, as well as in the periphery, are possible. Ligand binding to LRP1 can facilitate transcytosis of the blood brain barrier (56,57) and studies are underway to determine whether SP16 can cross the blood brain barrier.

Neuronal excitability was induced by capsaicin in both male and female mice. Importantly, SP16 and EI-tPA acutely reduced nociceptive behaviors associated with capsaicin. Capsaicin initiates activation of the neuronal transient receptor potential vanilloid 1 receptor (TRPV1) in small diameter neurons. LRP1 receptors are also located on small diameter DRG neurons (40), and accordingly it may de-activate other receptor systems such as TRPV1. Interactions between TRPV1 and TLR4 have been implicated in pain states (58) and EI-tPA (16) and SP16 appear to inhibit TLRs. Recently, it was shown that intraplantar injection of capsaicin induces spinal astrocytes in the superficial laminae (38). Specifically, Hes5+ spinal astrocytes appear to play a central role in gating brainstem descending control of hypersensitivity. Elucidating the key ascending and descending pain pathways modulated by SP16 may assist in refining targeted therapeutic development.

After peripheral nerve injury, Schwann cells dramatically upregulate LRP1 within 24 hrs predicting an early cellular target in the PNS (53). Accordingly, specialized cutaneous Schwann cells that are now known to initiate pain sensation (59) may play a role are consistent with their intimate association with unmyelinated c-fibers. In addition, pattern recognition receptors of innate immunity, including TLR4, are upregulated in Schwann cells. We showed that SP16 significantly reduced levels of TLR4 in nerve after injury. Since TLR4 is required for cytokine production (60) and macrophage recruitment, downregulation of receptors of innate immunity during nerve injury may serve as an underlying mechanism by which SP16 to regulates inflammatory cell recruitment. Another potential peripheral glia cell target are satellite cells in the DRG. Satellite cells express GFAP only after injury and are associated with peripheral sensitization (44). After PNL, we observed a significant increase in GFAP in DRGs that was blocked by SP16. Because satellite cell activation is involved in inflammatory cell hypersensitivity (44,45), it appears that SP16 antagonizes glia immune interactions that contribute to pain states.

Our novel findings reveal that LRP1 is likely a key regulator of innate immunity and inflammation in the PNS and are consistent with previous studies in other systems showing that membrane bound LRP1, and its activation supports anti-inflammatory activity. In leukocytes, LRP1 binds apoptotic cells that produces an anti-inflammatory signal (61). In microglia, deletion of LRP1 exacerbates experimental autoimmune encephalomyelitis in mice (19). SP16 blocked the expression of NFκβ induced by LPS in macrophage-like cells and blocked the formation of the inflammasome *in vitro* (11). In the injured sciatic nerve, SP16 reduced the levels of CD11b+ cells in both the sciatic nerve injury site and DRG two days following nerve ligation. CD11b+ populations include monocytes, macrophages (F480+/CD45+) and granulocytes (Ly6G+) in the injured nerve (62), thus we propose that SP16 regulates diverse inflammatory cell populations that are essential for pain alleviating activities. Interestingly, a recent study in a mouse model of colitis demonstrated that a single dose of EI-tPA (2μg/g), delivered after inflammation was established, improved colon health and disease progression, however, no changes in the number of CD45 positive leukocytes and F4/80 positive macrophages in the colon were noted (63). In contrast, SP16 reduced the number of CD45 positive cells at the infarct border zone in a mouse model of AMI, after a single dose of SP16 (100 μg) that was given within 30 minutes after reperfusion (11). Because LRP1 has diverse ligands with distinct circulating half-lives, binding affinities, co-receptors and tissue specificity, further studies are needed to help define optimal dosing routes and schedules for SP16.

Over the last several years, there have been substantial clues that LRP1 activation might play a role in alleviating pain states (17). These initial studies conclude that SP16 activates neuronal cell signaling in an LRP1 dependent manner and is capable of regulating both acute nociceptive pain and mechanical hypersensitivity, a key component of neuropathic pain. The translational implication of our findings are vast as novel pain treatments are urgently needed. Importantly, SP16 may serve as a therapeutic that prevents the transition from acute to chronic pain through its anti-nociceptive and anti-inflammatory activities.

ACKNOWLEDGMENTS

This work was supported by supported by a NIH/NINDS grant R01 NS097590 (to W.M.C) and by the Veterans Administration 1I01RX002484 (to W.M.C).

ABBREVIATIONS

AAT	α1-Antitrypsin
AMI	acute myocardial ischemia-reperfusion injury
DRG	dorsal root ganglia
EI-tPA	enzymatically inactive - tissue plasminogen activator
i.v.	intravenous
LRP1	low-density lipoprotein receptor-related protein-1
NMDA-R	N-methyl-D-aspartate receptor
PLL	poly-L-lysine
PNI	peripheral nerve injury
PNS	peripheral nerve system
PNL	partial nerve ligation
PWT	paw withdrawal thresholds
SCs	Schwann cells
s.c.	subcutaneous
TLRs	Toll-like receptors

REFERENCES

1. Jensen TS, Baron R, Haanpaa M, Kalso E, Loeser JD, Rice AS, Treed RD. A new definition of neuropathic pain. Pain. 2011;152(10):2204–2205. doi: 10.1016/j.pain.2011.06.017. [PubMed: 21764514]
2. Attal N Pharmacological treatments of neuropathic pain: The latest recommendations. Rev Neurol. 2019;175(1–2):46–50. doi:10.1016/j.neurol.2018.08.005. [PubMed: 30318260]
3. Volkow N, Benveniste H, McLellan AT. Use and misuse of opioids in chronic pain. Annu Rev Med. 2018;69:451–465. doi:10.1146/annurev-med-011817-044739. [PubMed: 29029586]
4. Lillis AP, Van Dyn LB, Murphy-Ullrich JE, Strickland DK. LDL receptor related protein 1: unique tissue-specific functions revealed by selective gene knockout studies. Physiol Rev. 2008;88(3):887–918. doi:10.1152/physrev.00033.2007. [PubMed: 18626063]
5. Gonias SL, Campana WM. LDL receptor-related protein-1: a regulator of inflammation in atherosclerosis, cancer, and injury to the nervous system. Am J Pathol. 2014;184(1):18–27. doi:10.1016/j.ajpath.2013.08.029. [PubMed: 24128688]
6. Joslin G, Fallon RJ, Bullock J, Adams SP, Perlmutter DH. The SEC receptor recognizes a pentapeptide neodomain of *a*1-Antitrypsin-protease complexes. J Biol Chem. 1991;266(17):11282–11288. doi:10.1016/S0021-9258(18)99160-X. [PubMed: 1645729]

7. Kounnas MZ, Church FC, Agraves WS, Strickland DK. Cellular internalization and degradation of anithrombin III-thrombin, heparin cofactor II-thrombin, and α1-Antitrypsin-trypsin complexes is mediated by the low-density lipoprotein receptor-related protein. J Biol Chem. 1996;271(11):6523–6529. doi:10.1074/jbc.271.11.6523. [PubMed: 8626456]

8. Arandjelovic S, Hall BD, Gonias SL. Mutation of lysine 1370 in full-length human alpha2-macroglobulin blocks binding to the low-density lipoprotein receptor-related protein-1. Arch Biochem Biophys. 2005;438(1):29–35. doi:10.1016/j.abb.2005.03.019. [PubMed: 15910735]

9. Migliorini MM, Behere EH, Brew S, Ingham KC, Strickland DK. Allosteric modulation of ligand binding to low density lipoprotein receptor related protein by the Receptor- associated Protein Requires Critical lysine residues with its carboy terminal domain. J Biol Chem. 2003;278(20):17986–17992. doi:10.1074/jbc.M212592200. [PubMed: 12637503]

10. Strickland DK, Muratoglu SC, Antalis TM. Serpin-enzymes receptors LDL receptor related protein 1 Methods Enzymol. 2011;499:17–31. doi:10.1016/B978-0-12-386471-0.00002-X. [PubMed: 21683247]

11. Toldo S, Austin D, Mauro AG, Mezzaroma E, Van Tassell BW, Marchetti C, Carbone S, Mogelsvang S, Gelber C, Abbate A. Low-density lipoprotein receptor-related protein-1 is a therapeutic target in acute myocardial infarction. JACC Basic Transl Sci. 2017;2(5):561–574. doi:10.1016/j.jacbts.2017.05.007. [PubMed: 30062170]

12. Potere N, Del Buono MG, Mauro AG, Abbate A, Toldo S. Low density lipoprotein receptor-related protein-1 in cardiac inflammation and infarct healing. Front Cardiovasc Med. 2019;6:51. doi:10.3389/fcvm.2019.00051. [PubMed: 31080804]

13. Wohlford GF, Buckley LF, Kadariya D, Park T, Chiabrando JG, Carbone S, Mihalick V, Halquist MS, Pearcy A, Austin D, Gelver C, Abbate A, Van Tassell B. A phase 1 clinical trial of Sp16, a first-in-class anti-inflammatory LRP1 agonist, in healthy volunteers. Plos One. 2021;16(5):e0247357. doi:10.1371/journal.pone.0247357. [PubMed: 33956804]

14. Mantuano E, Azmoon P, Brifault C, Banki MA, Gilder AS, Campana WM, Gonias SL. Tissue type plasminogen activator regulates macrophage activation and innate immunity. Blood. 2017;130(11):1364–1374. doi:10.1182/blood-2017-04-780205. [PubMed: 28684538]

15. Wen X, Xiao L, Zhong Z, Wang L, Li Z, Pan X, Liu Z. Astanthin acts via LRP-1 to inhibit inflammation and reverse lipopolysaccharide-induced M1/M2 polarization of microglial cells. Oncotarget. 2017;8(41):69370–69385. doi:10.18632/oncotarget.20628. [PubMed: 29050210]

16. Das L, Azmoon P, Banki M, Mantuano E, Gonias SL. Tissue-type plasminogen activator selectively inhibits multiple toll-like receptors in CSF-1-differentiated macrophages. PLoS One. 2019;14(11):e0224738. doi:10.1371/journal.pone.0224738. [PubMed: 31697716]

17. Bruno K, Woller SA, Miller YI, Yaksh TL, Wallace M, Beaton G, Chakravarthy K. Targeting toll-like receptor-4 (TLR4)-an emerging therapeutic target for persistent pain states. Pain. 2018;159(10):1908–1915. doi:10.1097/j.pain.0000000000001306. [PubMed: 29889119]

18. Luo X, Huh Y, Bang S, He Q, Zhang L, Matsuda M, Ji RR. Macrophage toll-like receptor 9 contributes to chemotherapy induced neuropathic pain in male mice. J Neurosci. 2019;39(35):6848–6864. doi:10.1523/JNEUROSCI.3257-18.2019. [PubMed: 31270160]

19. Chuang TY, Guo Y, Seki SM, Rosen AM, Johanson DM, Mandell JW, Lucchinetti CF, Gaultier A. LRP1 expression in microglia is protective during CNS autoimmunity. Acta Neuropath. 2016;4:68. doi:10.1186/s40478-016-0343-2.

20. Brifault C, Kwon H, Campana WM, Gonias SL. LRP1 deficiency in microglia blocks neuro-inflammation in the spinal dorsal horn and neuropathic pain processing. Glia. 2019;67(6):1210–1224. doi:10.1002/glia.23599. [PubMed: 30746765]

21. Quin KA, Pye VJ, Dai YP, Chesterman CN, Owensby DA. Characterization of the soluble form of the low-density lipoproteins receptor-related protein (LRP). Exp Cell Res. 1999;251(2):433–441. doi:10.1006/excr.1999.4590. [PubMed: 10471328]

22. Gorovoy M, Gaultier A, Campana WM Firestein GS, Gonias SL. Inflammatory mediators promote production of the LRP1/CD91 which regulates cell signaling and cytokine expression by macrophages. J Leuckoc Biol. 2010;88(4):769–778. doi:10.1189/jlb.0410220.

23. Orita S, Henry KW, Mantuano E, Yamauchi K, Ishikawa T, DeCorato A, Pollack M, Feltri ML, Wrabetz L, Ellisman M, Takahashi K, Gonias S, Campana WM. Schwann cell LRP1 regulates

Remak bundle ultrastructure and axonal interactions to prevent neuropathic pain. J Neurosci. 2013;33(13):5590–5602. doi:10.1523/jneurosci.3342-12.2013. [PubMed: 23536074]

24. Garcia-Fernandez P, Uceyler N, Sommer C. From the low-density lipoprotein receptor related protein 1 to neuropathic pain: a potentially novel target. Pain. 2021;6(1):e898. doi: 10.1097/PR9.0000000000000898.
25. Mantuano E, Lam MS, Gonias SL. LRP1 assembles unique co-receptor systems to initiate cell signaling in response to tissue-type plasminogen activator and myelin-associated glycoprotein. J Biol Chem. 2013;288(47):34009–34018. doi:10.1074/jbc.M113.509133. [PubMed: 24129569]
26. Yoon C, van Niekerk E, Henry K, Ishikawa T, Orita S, Tuszynski MH, Campana WM. Low-density lipoprotein receptor-related protein 1 (LRP1)-dependent cell signaling promotes axonal regeneration. J Biol Chem. 2013;288(37):26557–26568. doi:10.1074/jbc.M113.478552. [PubMed: 23867460]
27. Mattei V, Manganelli V, Martellucci S, Capozzi A, Mantuano E, Long A, Ferri A, Garafalo T, Sorice M, Misasi R. A multimolecular signaling complex including PrP^c and LPR1 is strictly dependent on lipid rafts and is essential for the function of tissue plasminogen activator. J Neurochem. 2020;152(4):468–481. doi:10.1111/jnc.14891. [PubMed: 31602645]
28. Shi Y, Mantuano E, Inoue G, Campana WM, Gonias SL. Ligand binding to LRP1 transactivates Trk receptors by a Src family kinase-dependent pathway. Sci Signal. 2009;2(68):ra18. doi:10.1126/scisignal.2000188. [PubMed: 19401592]
29. Herz J, Goldstein JL, Strickland DK, Ho YK, Brown MS. 39-kDa protein modulates binding of ligands to low density lipoprotein receptor-related protein/alpha 2-macroglobulin receptor. J Biol Chem. 1991;266(31):21232–21238. doi:10.1016/S0021-9258(18)54845-6. [PubMed: 1718973]
30. Mantuano E, Inoue G, Li X, Takahashi K, Gaultier A, Gonias SL, Campana WM. The hemopexin domain of matrix metalloproteinase-9 activates cell signaling and promotes migration of Schwann cells by binding to low-density lipoprotein receptor-related protein. J Neurosci. 2008;28(45):11571–11582. doi:10.1523/jneurosci.3053-08.2008. [PubMed: 18987193]
31. Sadri S, Hirosawa N, Le J, Romero H, Martellucci S, Kwon HJ, Pizzo D, Ohtori S, Gonias SL, Campana WM. Tumor necrosis factor receptor-1 is selectively sequestered into Schwann cell extracellular vesicles where it functions as TNFa decoy. Glia. 2021;1–17. doi:10.1002/glia.24098. epub ahead of print
32. Seltzer Z, Dubner R, Shir Y. A novel behavioral model of neuropathic pain disorders produced in rats by partial sciatic nerve injury. Pain. 1990;43(2):205–218. doi:10.1016/0304-3959(90)91074-S. [PubMed: 1982347]
33. Chaplan SR, Bach FW, Pogrel JW, Chung JM, Yaksh TL. Quantitative assessment of tactile allodynia in the rat paw. J Neurosci Methods. 1994;53(1):55–63. doi:10.1016/0165-0270(94)90144-9. [PubMed: 7990513]
34. Poplawski G, Ishikawa T, Brifault C, Lee-Kubli C, Regestam R, Henry KW, Shiga Y, Kwon H, Ohtori S, Gonias SL, Campana WM. Schwann cells regulate sensory neuron gene expression before and after peripheral nerve injury. Glia. 2018;66(8):1577–1590. doi:10.1002/glia.23325. [PubMed: 29520865]
35. Flutsch A, Henry K, Mantuano E, Lam MS, Shibiyama M, Takahashi K, Gonias SL, Campana WM. Evidence that LDL receptor-related protein 1 acts as an early injury detection receptor and activates c-Jun in Schwann cells. NeuroReport. 2016;27(18):1305–1311. doi:10.1097/WNR.0000000000000691. [PubMed: 27824728]
36. Albers GW, Bates VE, Clark WM, Bell R, Verro P, Hamilton SA. Intravenous tissue-type plasminogen activator for treatment of acute stroke: the Standard Treatment with Alteplase to Reverse Stroke (STARS) study. JAMA. 2000;283(9):1145–1150. doi:10.1001/jama.283.9.1145. [PubMed: 10703776]
37. Hunskaar S and Hole K. The formalin test in mice: dissociation between inflammatory and non-inflammatory pain. Pain. 1987;30(1):103–114. doi:10.1016/0304-3959(87)90088-1. [PubMed: 3614974]
38. Kohro Y, Matsuda T, Yoshihara K, Kohno K, Koga K, Katsuragi R, Oka T, Tashima R, Muneta S, Yamane T, Okada S, Momokino K, Furusho A, Hamase Km Oti T, Sakamoto H, Hayashida K, Kobayashi R, Hori T, TozakipSaitoh H, Mikoshiba K, Tayolor V, Inoue K, Tsuda M. Spinal astrocytes in superficial laminae gate brainstem descending control of mechanosensory

hypersensitivity. Nat Neurosci. 2020;23:1376–1387. doi:10.1038/s41593-020-00713-4. [PubMed: 33020652]

39. Holzer P Capsaicin: cellular targets, mechanisms of action, and selectivity for thin sensory neurons. Pharmacol Rev. 1991;43(2):143–201. [PubMed: 1852779]
40. Caterina MJ, Leffler A, Malmberg AB, Martin WJ, Trafton J, Petersen-Zeitz KR, Koltzenburg M, Basbaum AI, Julius D. Impaired nociception and pain sensation in mice lacking the capsaicin receptor. Science. 2000;288(5464):306–313. doi:10.1126/science.288.5464.306. [PubMed: 10764638]
41. Raoof R, Willemen HLDM, Eijkelkamp N. Divergent roles of immune cells and their mediators in pain. Rheumatology. 2018;57(3):429–440. doi:10.1093/rheumatology/kex308. [PubMed: 28968842]
42. Yu X, Liu H, Hamel KA, Morvan MG, Yu S, Leff J, Guan Z, Braz JM, Basbaum AI. Dorsal root ganglion macrophages contribute to both the initiation and persistence of neuropathic pain. Nat Commun. 2020;11(1):264. doi:10.1038/s41467-019-13839-2. [PubMed: 31937758]
43. Bravo-Caparrós I, Ruiz-Cantero MC, Perazzoli G, Cronin SJF, Vela JM, Hamed MF, Penninger JM, Baeyens JM, Cobos EJ, Nieto FR. Sigma-1 receptors control neuropathic pain and macrophage infiltration into the dorsal root ganglion after peripheral nerve injury. FASEB J. 2020;34(4):5951–5966. doi:10.1096/fj.201901921R. [PubMed: 32157739]
44. Avraham O, Deng PY, Jones S, Kuruvilla R, Semenkovich CF, Klyachko VA, Cavalli V. Satellite glial cells promote regenerative growth in sensory neurons. Nat Commun. 2020;11(1):4891. doi:10.1038/s41467-020-18642-y. [PubMed: 32994417]
45. Hanani M, Spray DC. Emerging importance of satellite glia in nervous system function and dysfunction. Nat Rev Neurosci. 2020;21(9):485–498. doi:10.1038/s41583-020-0333-z. [PubMed: 32699292]
46. Zhang H, Mei X, Zhang P, Ma C, White FA, Donnelly DF, LaMotte RH. Altered functional properties of satellite glial cells in compressed spinal ganglia. Glia. 2009;57(15):1588–1599. doi:10.1002/glia.20872. [PubMed: 19330845]
47. Old EA, Nadkarni S, Grist J, Gentry C, Bevan S, Kim KW, Mogg AJ, Perretti M, Malcangio M. Monocytes expressing CX3CR1 orchestrate the development of vincristine-induced pain. J Clin Invest. 2014;124(5):2023–2036. doi:10.1172/JCI71389. [PubMed: 24743146]
48. Long GL, Kjellber M, Villoutreix BO, Stenflo J. Probing plasma clearance of the thrombin-antithrombin complex with a monoclonal antibody against the totative serpin-enzyme complex receptor binding site. Eur J Biochem. 2003;270(20):4059–4069. doi:10.1046/j.1432-1033.2003.03793.x. [PubMed: 14519117]
49. Maekawa H, Tollefsen DM. Role of the proposed serpin-enzyme complex receptor recognition site in binding and internalization of thrombin-heparin cofactor II complex by hepatocytes. J Biol Chem. 1996; 271(31):18604–18609. doi:10.1074/jbc.271.31.18604. [PubMed: 8702511]
50. Van den Biggelaar M, Madsen JJ, Faber JH, Zuurveld MG, van der Zwaan C, Olsen OH, Stennicke HR, Mertens K, Meijer AB. Factor VIII interacts with the endocytic receptor low-density lipoprotein receptor-related protein 1 via an extended surface compromising “hot spot” lysine residues. J Biol Chem. 2015;290(27):16463–16476. doi:10.1074/jbc.M115.650911. [PubMed: 25903134]
51. Migliorini M, Li SH, Zhou A, Emal CD, Lawrence DA, Strickland DK. High affinity binding of plasminogen-activator inhibitor 1 complexes to LDL receptor-related protein 1 requires lysines 80,88, and 207. J Biol Chem. 295(1);212–222. doi: 10.1074/jbc.RA119.010449.
52. Patel S, Zhang X, Collins L, Fabre JW. A small, synthetic peptide for gene delivery via the serpin-enzyme complex receptor. J Gene Med. 2001;3(3):271–279. doi: 10.10002/jgm.180. [PubMed: 11437332]
53. Campana WM, Li X, Dragojlovic N, Janes J, Gaultier A, Gonias SL. The low-density lipoprotein receptor-related protein is a pro-survival receptor in Schwann cells: possible implications in peripheral nerve injury. J Neurosci. 2006;26(43):11197–11207. doi:10.1523/JNEUROSCI.2709-06.2006. [PubMed: 17065459]
54. Yamamoto T, Yaksh TL. Comparison of the antinociceptive effects of pre- and post-treatment with intrathecal morphine and MK801, an NMDA antagonist, on the formalin test in the

rat. Anesthesiology.1992;77(4):757–763. doi:10.1097/00000542-199210000-00021. [PubMed: 1416174]

55. Coderre TJ, Melzack R. The contribution of excitatory amino acids to central sensitization and peersistent nociception after formalin induced tissue injury. J Neurosci. 1992;12(9):3665–3670. doi:10.1523/jneurosci.12-09-03665.1992 [PubMed: 1326610]
56. Benchenane K, Berezowski V, Ali C, Fernández-Monreal M, López-Atalaya JP, Brillault J, Chuquet J, Nouvelot A, MacKenzie ET, Bu G, Cecchelli R, Touzani O, Vivien D. Tissue-type plasminogen activator crosses the intact blood-brain barrier by low-density lipoprotein receptor-related protein-mediated transcytosis. Circulation. 2005;111(17):2241–2249. doi:10.1161/01.CIR.0000163542.48611.A2. [PubMed: 15851587]
57. Demeule M, Currie J-C, Bertrand Y, Che C, Nguyen T, Regina A, Gabathuler R, Castaigne J-P, Beliveau R. Involvement of the low-density lipoprotein receptor related protein in the transcytosis of the brain delivery vector Angiopep-2. J Neurochem. 2008;106(4):1534–1544. doi:10.1111/j.1471-4159.2008.05492.x. [PubMed: 18489712]
58. Li Y, Adamek P, Zhang H, Tatsui CE, Rhines LD, Mrozkova P, Li Q, Kosturakis AK, Cassidy RM, Harrison DS, Cata JP, Sapire K, Zhang H, Kennamer-Chapman RM, Jawad AB, Ghetti A, Yan J, Palecek J, Dougherty PM. The cancer chemotherapeutic paclitaxel increases human and rodent sensory neuron responses to TRPV1 by activation of TLR4. J Neurosci. 2015;35(39):13487–13500. doi:10.1523/jneurosci.1956-15.2015. [PubMed: 26424893]
59. Abdo H, Calvo-Enrique L, Lopez JM, Song J, Zhang MD, Usokin D, Manira AE, Adameyko I, Hjerling-Leffler J, Ernfors P. Specialized cutaneous Schwann cells initiate pain sensation. Science. 2019;365(6454):695–699. doi:10.1126/science.aax6452. [PubMed: 31416963]
60. Hao HN, Peduzzi-Nelson JD, VandeVord PJ, Barami K, DeSilva SP, Pelinkovi D, Morawa LG: Lipopolysaccharide-induced inflammatory cytokine production by Schwann's cells dependent upon TLR4 expression. J Neuroimmunol. 2009;212(1–2):26–34. doi:10.1016/j.jneuroim.2009.04.020. [PubMed: 19525014]
61. Donnelly S, Roake W, Brown S, Young P, Nalik H, Wodsorth P, Isenberg DA, Reid KBM, Eggleton P. Impaired recognition of apoptotic neutrophils by the C1q/calreticulin and CD91 pathway in systemic lupus erythematosus. Arthritis and Rheumatology. 2006;54(5):1543–1556. doi:10.1002/art.21783.
62. Kalinski AL, Yoon C, Huffman LD, Duncker PC, Kohen R, Passino R, Hafner H, Johnson C, Kawaguchi R, Carbajal KS, Jara JS, Hollis E, Geschwind DH, Segal BM, Giger RJ. Analysis of the immune response to sciatic nerve injury identifies efferocytosis as a key mechanism of nerve debridement. eLife. 2020;9:e60223. doi:10.7554/eLife.60223. [PubMed: 33263277]
63. Das L, Banki MA, Azmoon P, Pizzo D, Gonias SL. Enzymatically inactive tissue-type plasminogen activator reverse disease progression in the dextran sulfate sodium mouse model of inflammatory bowel disease. Am J Pathol. 2021;191(4):590–601. doi:10.1016/j.ajpath.2021.01.001. [PubMed: 33465348]

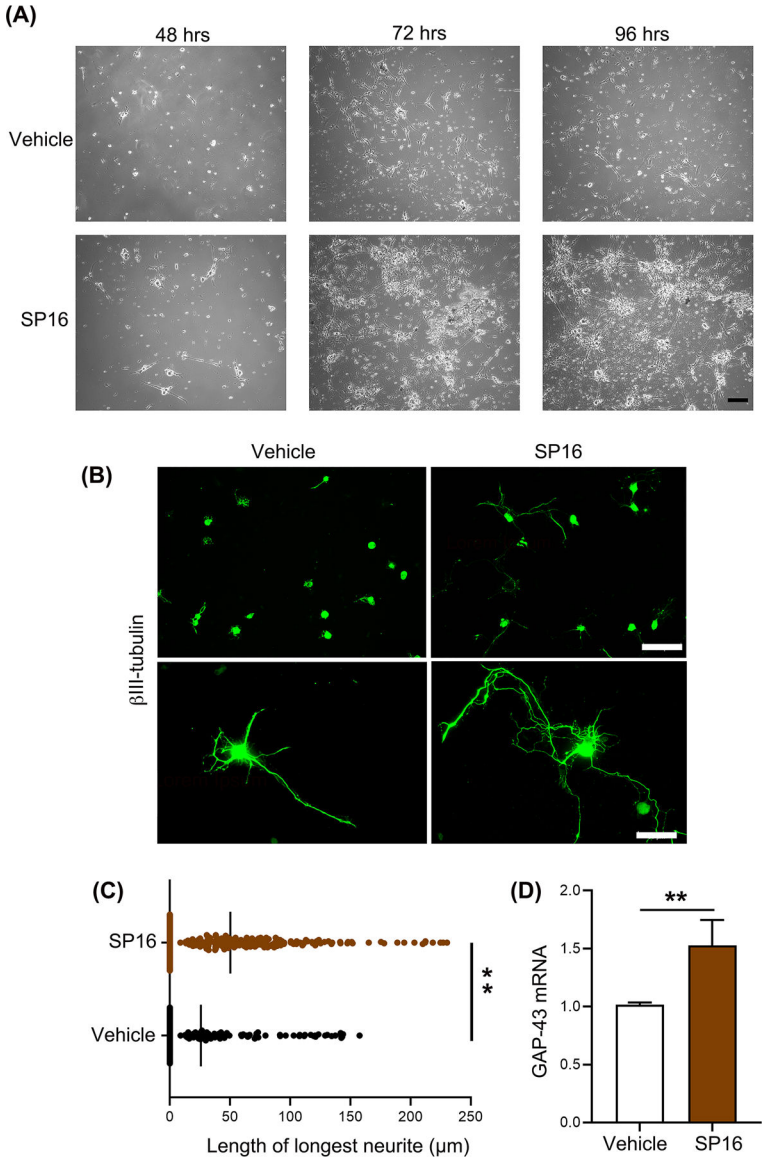

Figure 1. SP16 promotes neurite length and growth associated protein-43 (GAP-43) in adult primary rat DRG neurons.

(A) Representative phase contrast images of primary adult DRG neurons cultured over time. Cultures were treated with vehicle or SP16 (100 ng/mL) daily for 48, 72, and 96 hrs. Scale bar 500 μm. **(B)** Representative image of immunofluorescence to detect βIII-Tubulin in primary cultured adult DRG neurons in control and SP16 (240 nM) treated cells after 54 hrs. Upper panel: scale bar 200 μm; lower panel: scale bar 50 μm. Note extensive neurite length in SP16 treated neurons. **(C)** Quantification of immunofluorescence analysis in control (n=144 neurons) and SP16 (n=222 neurons) samples obtained from 11 distinct cultures. SP16 significantly increased maximum neurite length compared to controls. Mann-Whitney test, sum of ranks in vehicle and SP16 treated: 23537,43625; ** P<0.01. Data are expressed as mean ± SEM. **(D)** Primary cultured adult DRG neurons were treated with vehicle or SP16 (240 nM) for 24 hrs. RT-qPCR analysis of GAP-43 mRNA levels (n=8 independent

studies). SP16 significantly increased the regenerative associated gene compared to vehicle. Mann-Whitney test, sum of ranks in vehicle or SP16: 29,76, $^{**}P < 0.01$.

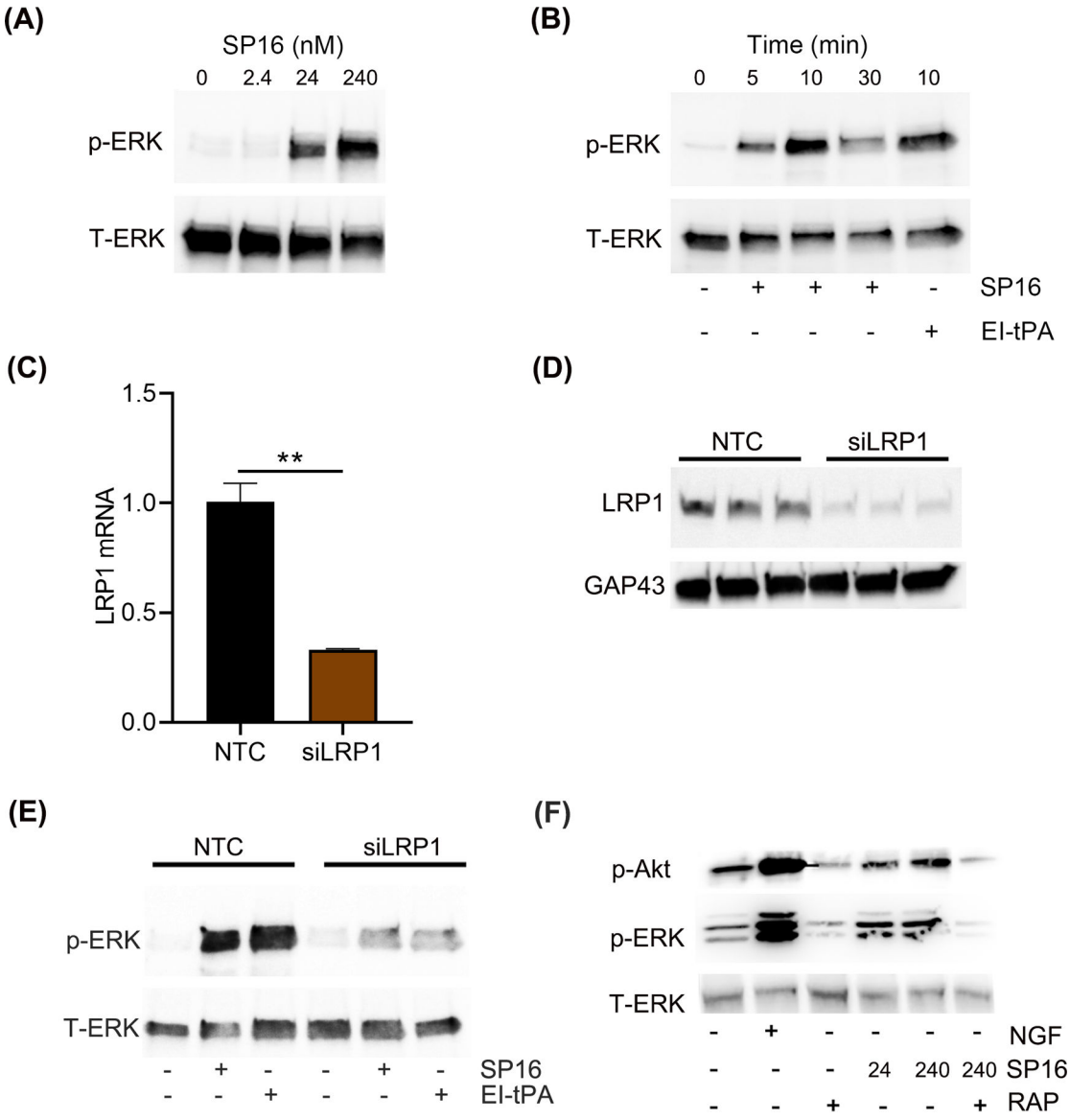

Figure 2. In PC12 cells, SP16 activates transient cell signaling in an LRP1 dependent manner.

(A) Dose dependent (0–240 nM) activation of phospho-ERK1/2 by SP16 after 10 min. **(B)** Timecourse (0–30 min) of SP16 (240 nM) activation of phospho-ERK1/2. Last lane (far right) shows activation of phospho-ERK1/2 by a known LRP1 agonist, EI-tPA (12 nM). Equal amounts of protein lysates (20 μg) were loaded per lane. Immunoblot analysis detects phopsho-ERK1/2 and total ERK1/2, as a loading control. **(C)** RT-qPCR analysis of LRP1 mRNA after transfection with LRP1 siRNA for 48 h. Data are presented as mean ± SEM; n=3 independent experiments. T-test, T=8.024, df=4, ** P<0.05. **(D)** Immunoblot of LRP1 levels in PC12 cells transfected with non-targeting controls (NTC) or siLRP1 for 48 hrs in PC12 cells. **(E)** Representative immunoblot of phospho-ERK1/2 activated by SP16 (240 nM) over time 48 hrs after transfection with NTC or siLRP1. **(F)** Immunoblot showing activation of phospho-Akt and phospho-ERK1/2 with vehicle or SP16 (24 or 240 nM) for 10 mins and in some wells, pretreated with RAP (150 nM) for 15 min. NGF (0.36 nM) for 10

min served as a cell signaling control. Equal amounts of protein lysates (20 μg) were loaded per lane. Total ERK served as a loading control.

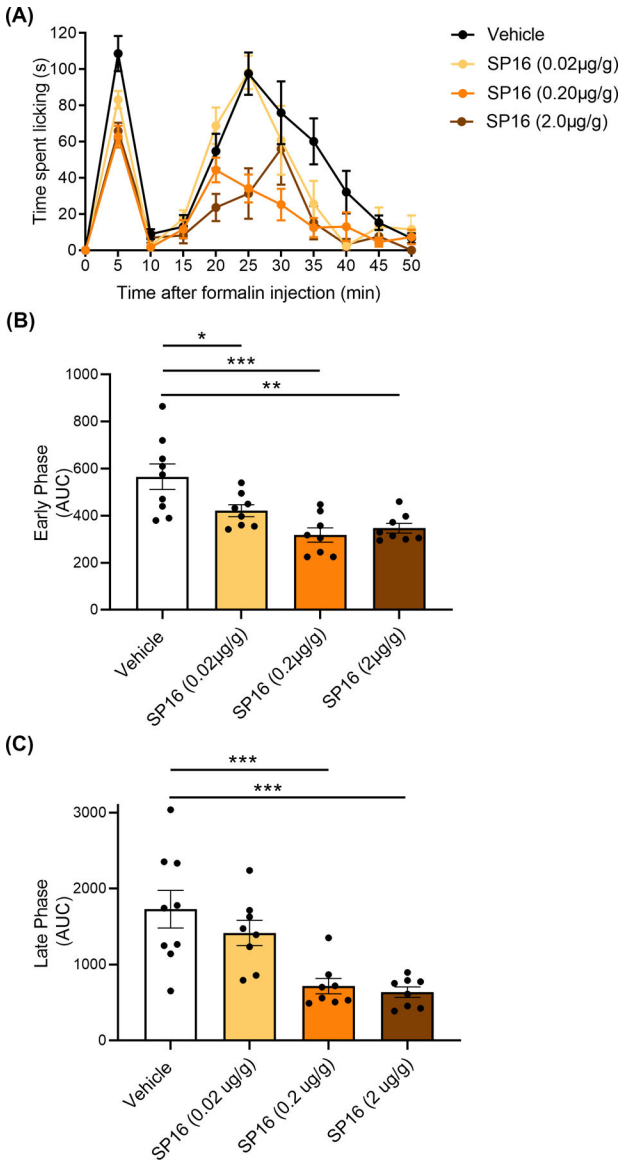

Figure 3. SP16 modulates both early and late phase of the formalin test.

(A) Time-course of formalin (2.5%) induced paw licking in C57BL6 mice. Vehicle or SP16 (0–2 μg/g s.c.) was given 1 hr prior to formalin injection into the hind paw. **(B)** Quantification of area under the curve (AUC) for vehicle and SP16 (0.02, 0.2 and 2 μg/g) during the early phase. Data are expressed as mean ± SEM; One-way ANOVA, F=9.523, ***P<0.001. Tukey's *post hoc* test, vehicle (n=9) *vs.* SP16 0.02 μg/g (n=8), *P<0.05; vehicle *vs.* SP16 0. 2 μg/g (n=8), ***P< 0.001; vehicle *vs.* SP16 2.0 μg/g (n=8), **P< 0.01. **(C)** Quantification of area under the curve (AUC) for vehicle and SP16 (0.02, 0.2 and 2 μg/g) during the late phase. Data are expressed as mean ± SEM; One-way ANOVA, F=10.2, ****P<0.0001. Tukey's *post hoc* test, vehicle (n=9) *vs.* SP16 0.02 μg/g (n=8), P=ns; vehicle *vs.* SP16 0. 2 μg/g (n=9), ***P<0.005; vehicle *vs.* SP16 2.0 μg/g (n=8), ***P< 0.005.

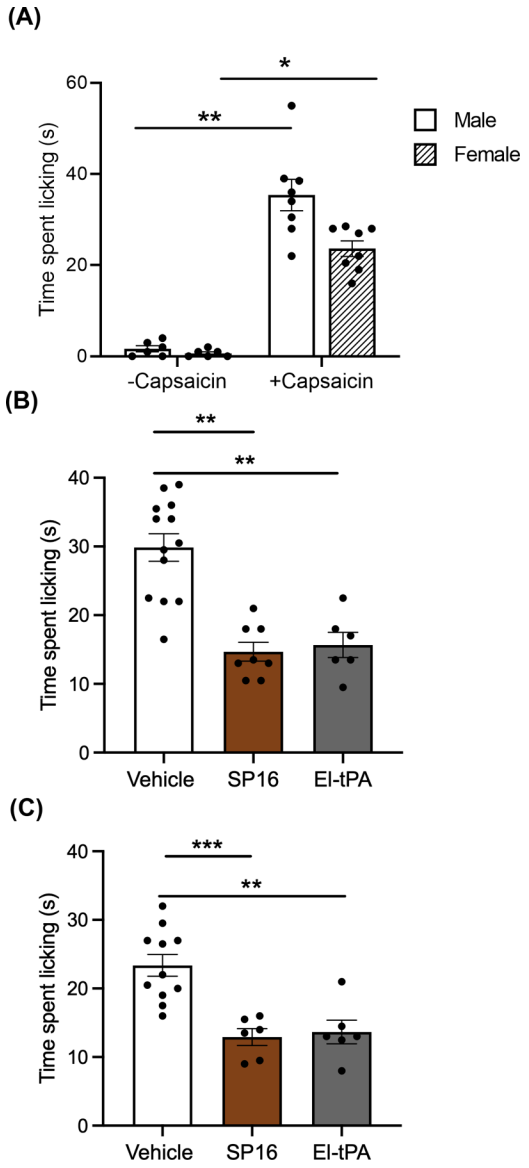

Figure 4. Systemically administered SP16 and EI-tPA attenuates acute nociception induced by intraplantar capsaicin.

(A) Nociceptive related behaviors (time spent licking) increased in both male and female mice after intraplantar injection of capsaicin (20 μg) when compared to vehicle (cyclodextrin: 20%). Data are expressed as mean ± SEM. Kruskal-Wallis test ****P<0.0001. Dunn's multiple comparisons test *post hoc* test male *vs.* female without capsaicin (n=6), P=ns; male *vs.* female with capsaicin (n=8), P=ns; male without capsaicin *vs.* male with capsaicin **P<0.01; female without capsaicin *vs.* female with capsaicin *P<0.5. **(B)** Nociceptive related behaviors (time spent licking) after administration of LRP1 interactors, SP16 (2 μg/g) or EI-tPA (2 μg/g) in male mice with intraplantar capsaicin over 10 minutes. Data are mean ± SEM. One-way ANOVA, F=21.28 ***P<0.001. Tukey's *post hoc* test, vehicle (n=13) *vs.* SP16 (n=8), **P<0.01; vehicle *vs.* EI-tPA (n=6), **P<0.01; **(C)** Nociceptive related behaviors (time spent licking) after administration of LRP1 interactors, SP16 (2 μg/g) or EI-tPA (2 μg/g) in female mice with intraplantar capsaicin over 10 minutes.

Data are mean ± SEM. One-way ANOVA, F=14.20 ***P<0.005. Tukey's *post hoc* test, vehicle (n=13) *vs.* SP16 (n=8), ***P<0.005; vehicle *vs.* EI-tPA (n=6), **P<0.01.

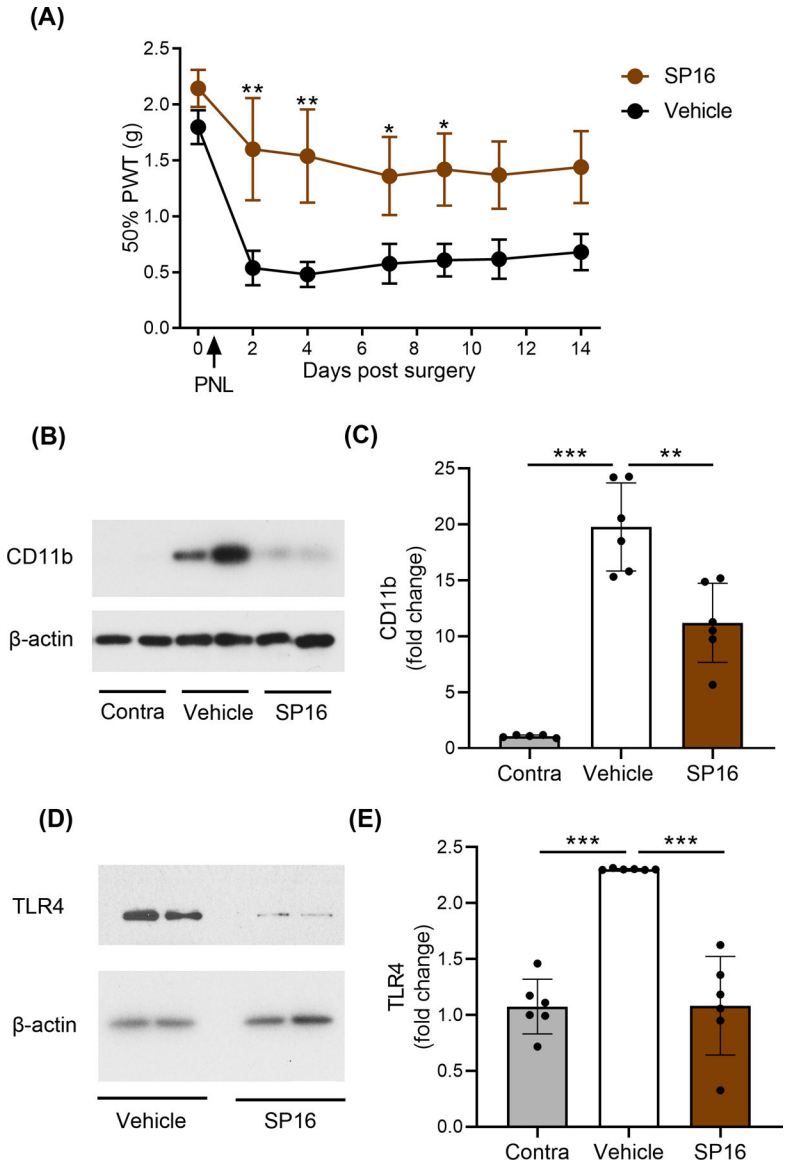

Figure 5. Systemically administered SP16 treatment blocks the development of mechanical hypersensitivity and inflammatory cell recruitment after PNL.

(A) Tactile allodynia develops after PNL and are sustained for 14 days. SP16 (2 μg/6) delivered daily and subcutaneously significantly prevented the development of tactile allodynia for 9 days post-injury (***P*<0.01). Data are expressed as mean ± SEM (n=7 mice/group). Two-way ANOVA, days (main effect) F(6,42)=2.51, **P*<0.05; treatment (main effect) F(1,42)=57.91, *****P*<0.0001; treatment × day (interaction) F(6,42)=0.7512 *P*=ns. Sidak's multiple comparison test vehicle *vs.* SP16 post injury, day 2 ***P*<0.01, day 4 ***P*<0.01, day 7 **P*<0.05, day 9 **P*<0.05. **(B,D)** Immunoblot analysis of injured sciatic nerve two days after PNL in vehicle and SP16 treated mice. SP16 treatment reduced inflammatory cell infiltration (CD11b) and suppressed TLR4. **(C)** Densitometric analysis of CD11b. One-way ANOVA, F=39.05; *****P*<0.0001, Tukey's *post hoc* test, contra (n=5) *vs.* vehicle (n=6) ****P*<0.005, vehicle *vs.* SP16 (n=5) ***P*<0.01. **(E)** Densitometric analysis of TLR4. One-way ANOVA, F=18.54; *****P*<0.0001, Tukey's *post hoc* test contra (n=6) *vs.*

vehicle (n=6), ***P<0.005 vehicle *vs.* SP16 (n=6) ****P*<0.005) All data are expressed as mean ± SEM.

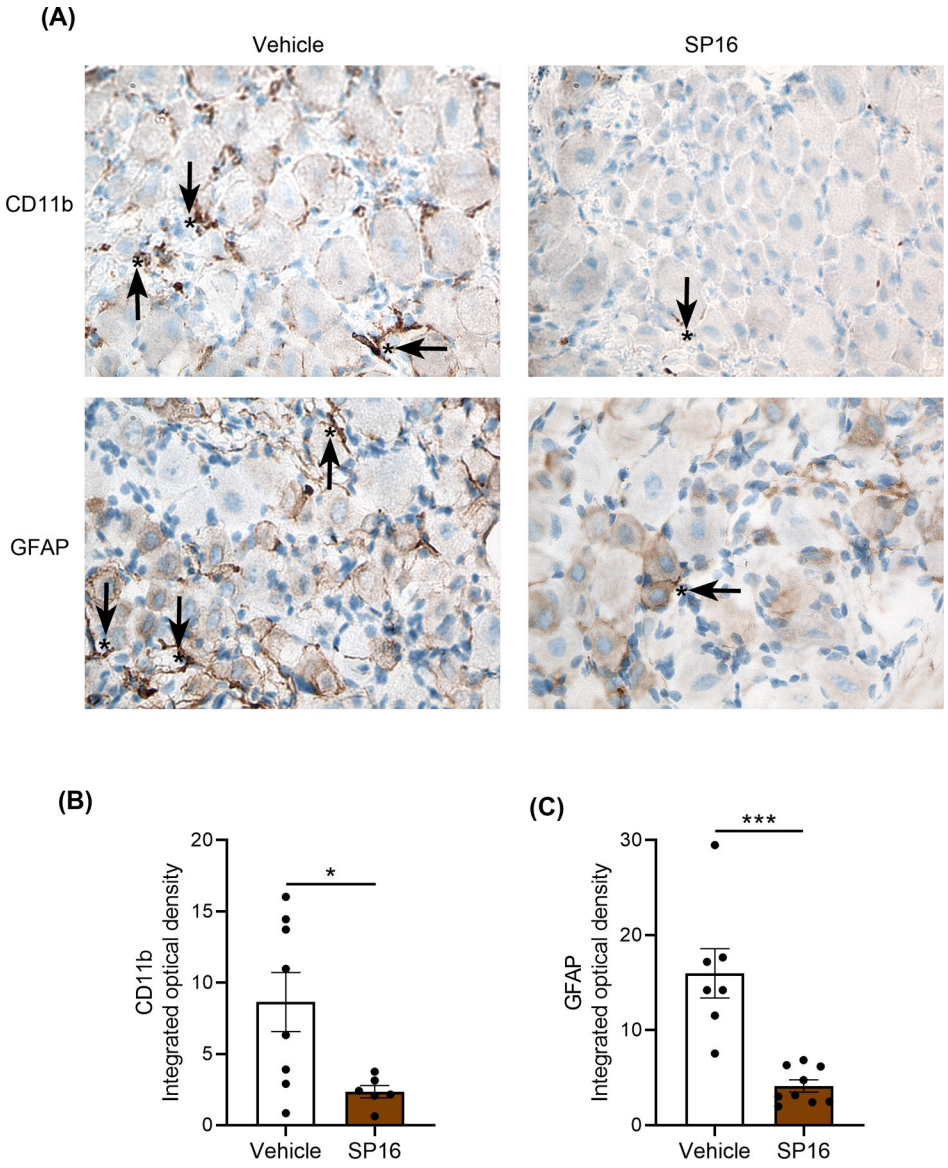

Figure 6. Inflammatory cell recruitment and satellite cell activation are reduced by SP16 after PNL.

(A) Transverse sections of L4 DRG immunostained for CD11b and GFAP after vehicle or SP16 treatment two days post PNL. Note abundant immunoreactivity (brown) identifying CD11b (black arrows, upper panels) in between neuronal cell bodies and close to blood vessels or identifying GFAP (black arrows, lower panels) surrounding the neuronal cell bodies in injured vehicle-treated (left) or SP16-treated DRGs (right). CD11b and GFAP immunoreactivity in SP16 treated DRGs are minimal. Nuclei are stained with hematoxylin (blue). **(B)** Quantification of CD11b in DRGs. Mann-Whitney test, sum of ranks in vehicle and SP16 treated: 23537,43625; ** $P<0.01$. Data are expressed as mean ± SEM. Mann Whitney U test, sum of ranks in vehicle (n=8) and SP16 (n=6): 77, 28; * $P<0.05$. **(C)** Quantification of GFAP in DRGs. Mann Whitney U test, sum of ranks in vehicle (n=7) and SP16 (n=9): 91, 45; *** $P<0.005$.